MODIFICATION OF PROTEIN MICELLES BY LIMITED HYDROLYSIS OF PEPTIDE BONDS: A MODEL OF THE SEQUENTIAL DEGRADATION OF β-CASEIN MICELLES

Cite this: *INEOS OPEN*, **2023**, *6 (2)*, 44–48
DOI: 10.32931/io2313a

Received 13 October 2023,
Accepted 26 November 2023

http://ineosopen.org

A. V. Golovanov,[a] G. Güler,[b] and M. M. Vorob'ev*[a]

[a] *Nesmeyanov Institute of Organoelement Compounds, Russian Academy of Sciences, ul. Vavilova 28, str. 1, Moscow, 119334, Russia*
[b] *Biophysics Laboratory, Department of Physics, Izmir Institute of Technology, Urla, 35430 Izmir, Turkey*

Abstract

A model for the degradation of β-casein micelles with the limited hydrolysis of trypsin-specific peptide bonds was proposed. A sequential mechanism of the degradation of micelles and assembly of peptide nanoparticles from the fragments of a β-casein polypeptide chain was considered. The degradation kinetics was studied by numerical modeling, taking into account the formation of intermediate components of different sizes and peptide nanoparticles, which are more difficult to hydrolyze with trypsin. The simulation results are consistent with the experimental data previously obtained by atomic force microscopy, FTIR spectroscopy, and light scattering.

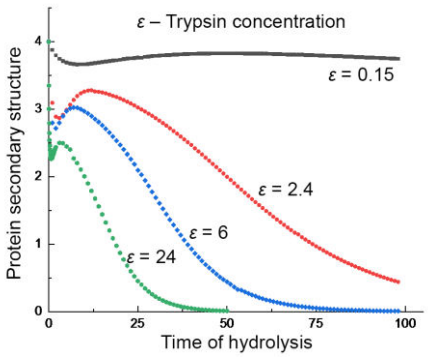

Key words: peptide nanoparticles, kinetic model, β-casein hydrolysis by trypsin.

Introduction

β-Casein micelles are used as transport systems for hydrophobic drug molecules which are concentrated in a hydrophobic center of the micelles [1, 2]. For example, the use of β-casein micelles for transporting the anticancer drug paclitaxel as well as D group vitamins has been well studied [3, 4]. Limited enzymatic hydrolysis of casein proteins affords modified casein micelles of various sizes [5], which can also be used as transport systems. The hydrolysis of proteins that form micelles must be controlled, since the sizes of the modified micelles change during hydrolysis [6–8]. To obtain the required micelles, it is necessary to know the kinetic regularities of the enzymatic hydrolysis of proteins in order to determine the point at which it is necessary to stop the hydrolysis by inhibiting a proteolytic enzyme.

β-Casein micelles are soap-like micelles formed by dispersing one fraction of casein proteins isolated from a complex of α-, β-, and κ-caseins. From a physicochemical point of view, the formation of thermodynamically stable β-casein micelles is described by the Kegel model, which is consistent with the physicochemical data obtained from differential scanning calorimetry, atomic force microscopy (AFM), and static light scattering studies [9–11]. We changed the physicochemical characteristics of micelles during the hydrolysis of β-caseins by trypsin using AFM, IR spectroscopy, and static light scattering [8, 12, 13]. Among the results obtained, of note is a nonmonotonic change in secondary structures of a polypeptide chain (α-helices and β-sheets) during the hydrolysis of β-casein micelles by trypsin [14], although the simplest model for the degradation of protein structures assumes a monotonic decrease in the secondary structure during the hydrolysis of proteins and polypeptide chains. We explained this interesting phenomenon using a simplified model of the degradation of protein micelles by the intermolecular interaction of the fragments of a β-casein polypeptide chain and the formation of new nanoparticles, which are released during the hydrolysis of the initial micelles [14].

Earlier we carried out a simplified modeling of the degradation of protein micelles under the action of proteolytic enzymes [14]. It was suggested that during degradation β-casein micelles first disintegrate into fragments, then these fragments are assembled into new particles, and only then the latter are finally hydrolyzed to form lower peptides. It was assumed that the enzyme concentration remains unchanged during hydrolysis; therefore, the differential equations for the system components were linear and the concentration dependences for them were obtained in an analytical form.

The goal of this work was to construct a model for the degradation of β-casein micelles during limited hydrolysis of polypeptide chains, taking into account the enzyme inhibition during hydrolysis as well as several types of hydrolyzed micelles, differing in size and degree of hydrolysis. These assumptions differ from the conditions conjectured when constructing the simplified models [14, 15] and correspond more realistically to the experimental data on the degradation of β-casein micelles that have been obtained recently [6, 7, 14]. These complications of the model require the use of numerical modeling, since a complex model cannot be described in an analytical form.

Results and discussion

The micelle degradation model is represented by the

following kinetic scheme shown below:

$$\begin{cases} M \xrightarrow{k_1 E} X_3 \xrightarrow{k_2} Y_3 + Y_1 \\ \qquad\quad {\scriptstyle k_z X_2}\downarrow \\ \qquad\quad\; Z \\ Y_3 \xrightarrow{k_3 E} X_2 \xrightarrow{k_2} Y_2 + Y_1 \\ \qquad\quad {\scriptstyle k_z X_3}\downarrow \\ \qquad\quad\; Z \\ Y_2 \xrightarrow{k_3 E} X_1 \xrightarrow{k_2} 2Y_1 \\ Y_1 \xrightarrow{k_4 E} P, \end{cases} \qquad (1)$$

where M are the initial micelles consisting of four blocks, one of which can be hydrolyzed by the enzyme with a rate constant k_1E. The original micelles are converted into hydrolyzed micelles X_3 featuring three non-hydrolyzed blocks and one hydrolyzed block, and then hydrolyzed micelles X_3 break down into smaller micelles Y_3, containing non-hydrolyzed blocks, and peptide nanoparticles Y_1, containing the fragments of a β-casein polypeptide chain. Y_1 particles are similar to new particles Y that we described earlier when constructing a simplified model [14]. Peptide particles Y_1 are formed by aggregated peptide fragments, which provide a higher density of these particles compared to the initial micelle [6, 7]. They can be hydrolyzed with a rate constant k_4E, and subsequently particles Y_1 disappear as macromolecular particles detected by light scattering and AFM. Micelles Y_3 are converted into hydrolyzed micelles X_2 with two non-hydrolyzed blocks and one hydrolyzed block. Then they are converted into smaller micelles Y_2 and peptide particles Y_1. In small micelles Y_2, consisting of two blocks, the hydrolysis occurs in the whole micelle at once, resulting in hydrolyzed micelle X_1, which splits into two particles Y_1.

The non-enzymatic stages of the process, occurring with a rate constant k_2, in addition to the dissociation of the non-hydrolyzed and hydrolyzed parts of the micelle, also include the assembly of peptide fragments that leads to the formation of Y_1 nanoparticles. Then they hydrolyze with a rate constant k_4E. Hydrolyzed micelles X_3 and X_2 aggregate with a second-order rate constant k_z to form large modified micelles Z with a diameter greater than 100 nm, which we studied by AFM [6–8].

For scheme (1), the following system of nine ordinary nonlinear differential equations is valid that reflects the kinetics of the process:

$$\begin{cases} \dfrac{dM}{dt} = -k_1EM \\ \dfrac{dX_1}{dt} = k_3EY_2 - k_2X_1 \\ \dfrac{dX_2}{dt} = k_3EY_3 - k_2X_2 - k_zX_2X_3 \\ \dfrac{dX_3}{dt} = k_1EM - k_2X_3 - k_zX_2X_3 \\ \dfrac{dY_1}{dt} = k_2\left(2X_1 + X_2 + X_3\right) - k_4EY_1 \\ \dfrac{dY_2}{dt} = k_2X_2 - k_3EY_2 \\ \dfrac{dY_3}{dt} = k_2X_3 - k_3EY_3 \\ \dfrac{dZ}{dt} = k_zX_2X_3 \\ \dfrac{dP}{dt} = k_4EY_1. \end{cases} \qquad (2)$$

The components included in the model differ in size (mass): the size of M and X_3 is 4 blocks, the size of X_2 and Y_3 is 3 blocks, the size of X_1, Y_2 is 2 blocks, the size of Y_1, P is 1 block, and the size of Z is 7 blocks. The material balance equation can be written for the concentration of blocks that make up the micelles, which is four times higher than the initial concentration of micelles S_0:

$$4S_0 = 4M + 2X_1 + 3X_2 + 4X_3 + Y_1 + 2Y_2 + 3Y_3 + 7Z + P. \qquad (3)$$

Enzyme E is involved in the hydrolysis of peptide bonds and is inhibited by the hydrolysis products; therefore, the concentration of the active enzyme decreases as the concentration of the hydrolyzed micelles increases. We observed a decrease in the concentration of the active enzyme during hydrolysis by a decrease in the rate of hydrolysis of peptide bonds [5]. In our model, the concentration of active enzyme E is given by the following empirical equation:

$$E = \frac{\varepsilon E_0}{1 + \dfrac{S_0}{K_\mathrm{M}} + \gamma\left(x_2 + x_3\right)}, \qquad (4)$$

where E_0 is the standard enzyme concentration (E_0 = 1 μg/mL), ε is a dimensionless factor indicating how many times the chosen enzyme concentration differs from the standard one, K_M is the apparent Michaelis constant, γ is the dimensionless parameter that determines the enzyme inhibition by the reaction products, $x_2 = X_2/S_0$, $x_3 = X_3/S_0$. K_M and γ are associated with the enzyme saturation with the hydrolysis products.

The system of differential equations (2) can be presented in the following dimensionless form:

$$\begin{cases} \dfrac{dm(\tau)}{d\tau} = -\varepsilon m(\tau) \\ \dfrac{dx_1(\tau)}{d\tau} = \kappa_3\varepsilon y_2(\tau) - \kappa_2 x_1(\tau) \\ \dfrac{dx_2(\tau)}{d\tau} = \kappa_3\varepsilon y_3(\tau) - \kappa_2 x_2(\tau) - \kappa_z x_2(\tau)x_3(\tau) \\ \dfrac{dx_3(\tau)}{d\tau} = \varepsilon m(\tau) - \kappa_2 x_3(\tau) - \kappa_z x_2(\tau)x_3(\tau) \\ \dfrac{dy_1(\tau)}{d\tau} = \kappa_2[2x_1(\tau) + x_2(\tau) + x_3(\tau)] - \kappa_4\varepsilon y_1(\tau) \\ \dfrac{dy_2(\tau)}{d\tau} = \kappa_2 x_2(\tau) - \kappa_3\varepsilon y_2(\tau) \\ \dfrac{dy_3(\tau)}{d\tau} = \kappa_2 x_3(\tau) - \kappa_3\varepsilon y_3(\tau) \\ \dfrac{dz(\tau)}{d\tau} = \kappa_z x_2(\tau)x_3(\tau) \\ \dfrac{dp(\tau)}{d\tau} = \kappa_4\varepsilon y_1(\tau), \end{cases} \qquad (5)$$

where $m = M/S_0$, $x_1 = X_1/S_0$, $x_2 = X_2/S_0$, $x_3 = X_3/S_0$, $y_1 = Y_1/S_0$, $y_2 = Y_2/S_0$, $y_3 = Y_3/S_0$, $z = Z/S_0$, $p = P/S_0$, $\tau = k_1E_0t$, $\kappa_2 = k_2/k_1E_0$, $\kappa_3 = k_3/k_1$, $\kappa_4 = k_4/k_1$, $\kappa_z = k_zS_0/k_1E_0$.

Systems (2) and (5) are written under the conditions γ = 0 and S_0/K_M = 0 to avoid cluttered appearance.

The material balance equation for (5) has the following form:

$$4 = 4m + 2x_1 + 3x_2 + 4x_3 + y_1 + 2y_2 + 3y_3 + 7z + p. \qquad (6)$$

To solve the system of differential equations (5), it is necessary to set the initial conditions in the form:

$$m|_{\tau=0} = 1,\ x_1|_{\tau=0} = x_2|_{\tau=0} = x_3|_{\tau=0} = \\ = y_1|_{\tau=0} = y_2|_{\tau=0} = y_3|_{\tau=0} = z|_{\tau=0} = p|_{\tau=0} = 0\,. \qquad (7)$$

Since system (5) is nonlinear, it was solved numerically. The solutions are functions of concentrations *vs* time (Fig. 1). The following numerical values of the coefficients were used for the calculations: $\kappa_2 = 0.2$, $\kappa_3 = 0.1$, $\kappa_4 = 0.03$, $\kappa_z = 0.1$, $S_0/K_M = 1$, $\gamma = 5$.

The course of the curves (Fig. 1) corresponds to the sequential transformation of the initial micelles m into intermediate products x and y, which are first accumulated and then are consumed. The final products are peptides p and large particles z, which, in our opinion, are not hydrolyzed.

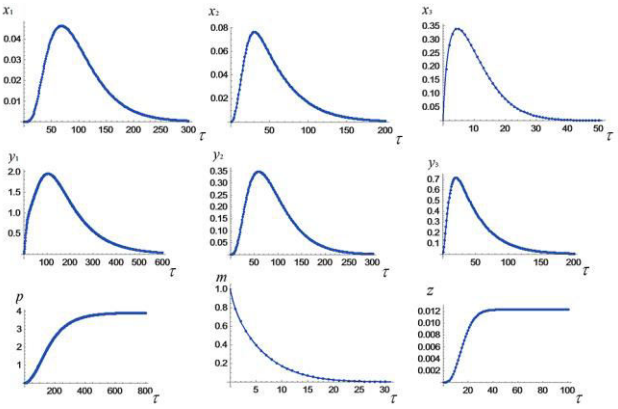

Figure 1. Results of the numerical solution of the system of equations (5) at $\varepsilon = 0.6$.

Earlier we used static light scattering to describe the kinetics of the degradation of casein micelles [12, 13]. Using the static scattering dissymmetry method, two key parameters were determined: the total molar concentration of light-scattering particles (I_{45}) and particle size (I_{45}/I_{135} ratio), where I_{45} and I_{135} are the light scattering intensities at angles of 45° and 135°, respectively [16–19]. However, it should be noted that the dissymmetry ratio can be used only for an approximate estimation of the size of protein particles [18, 19]. An example of the experimental dependences of the change in the number of particles (I_{45}) and particle size (I_{45}/I_{135}) during hydrolysis is presented in Fig. 2a [12, 13]. An example of the changes in the number of particles ($A = m + x_1 + x_2 + x_3 + y_1 + y_2 + y_3 + z$) and particle size (average number of blocks in particles, $l = B/A$, $B = 4m + 2x_1 + 3x_2 + 4x_3 + y_1 + 2y_2 + 3y_3 + 7z$) predicted by the model as a function of hydrolysis duration is presented in Fig. 2b at $\varepsilon = 0.6$ and Fig. 2c at $\varepsilon = 6$.

Figures 2a–c show the qualitative agreement between the results of the numerical modeling and the experimental data: the course of curves A and l *vs* hydrolysis time is approximately the same. Depending on the values of ε, the curves shift. For example, at high values of ε, the maximum number of particles and the minimum particle size l are achieved at shorter hydrolysis times. However, due to the large number of parameters, it is difficult to accurately determine the values of the parameters (for example, rate constants) from the shape of curves $A(\tau)$ and $l(\tau)$.

To evaluate the changes in the secondary structure during the hydrolysis of micelles, it is necessary to make assumptions

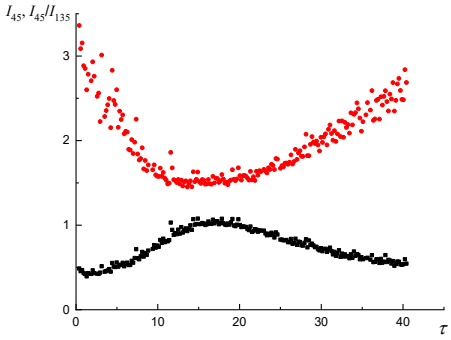

Figure 2a. Typical time course of the number of light-scattering particles I_{45} (■) and their size I_{45}/I_{135} (●) during the hydrolysis of β-casein micelles with trypsin [12, 13]. I_{45} is the total molar concentration of light-scattering particles; I_{45}/I_{135} is the particle size; τ is the dimensionless time. β-Casein concentration was 1 g/L, trypsin concentration was 0.001 g/L, the temperature was 43 °C.

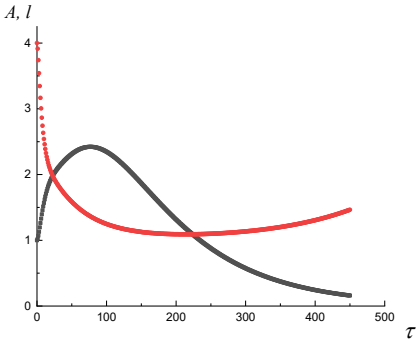

Figure 2b. Results of the numerical modeling of the dependences of the number of particles A (■) and particle size (average number of blocks in particles, $l = B/A$, ●) on the dimensionless hydrolysis time at $\varepsilon = 0.6$. τ is the dimensionless time.

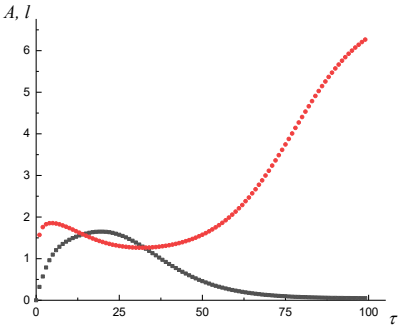

Figure 2c. Results of the numerical modeling of the dependences of the number of particles A (■) and particle size (average number of blocks in particles, $l = B/A$, ●) on the dimensionless hydrolysis time at $\varepsilon = 6$. τ is the dimensionless time.

about which components of the model (M, X, Y) retain the secondary structure and which lose it as a result of hydrolysis of peptide bonds. As well as in the previous report [14], we assume that the secondary structures (α-helices, β-sheets) in particles Y (Y_3, Y_2, and Y_1) are preserved. If the concentration of the secondary structures in the initial micelles is $4M$, then the concentrations of the secondary structures in particles Y_3, Y_2, and Y_1 will be $3Y_3$, $2Y_2$, and Y_1, respectively, given the sizes of these particles. As well as in the previous report [14], we assume that particles X lose half of their secondary structures. Thus, the

concentrations of the secondary structures in particles X_3, X_2, and X_1 will be $2X_3$, $3/2X_2$, and $X1$, respectively, given the sizes of these particles. Therefore, in a dimensionless form, the concentration of the secondary structures is determined by the following formula:

$$W = 4m + x_1 + \frac{3}{2}x_2 + 2x_3 + y_1 + 2y_2 + 3y_3. \quad (8)$$

The dependences of W on hydrolysis time for three enzyme concentrations are presented in Fig. 3. As the enzyme concentration decreases, the local concentration maximum of the secondary structures shifts toward longer hydrolysis times. This pattern was observed when we determined the concentrations of α-helices and β-sheets using FTIR spectroscopy [14]. The application of the model that implies the sequential degradation of the initial micelles with the formation of new particles and their subsequent degradation gave the same result as was obtained earlier with a simple linear model [14].

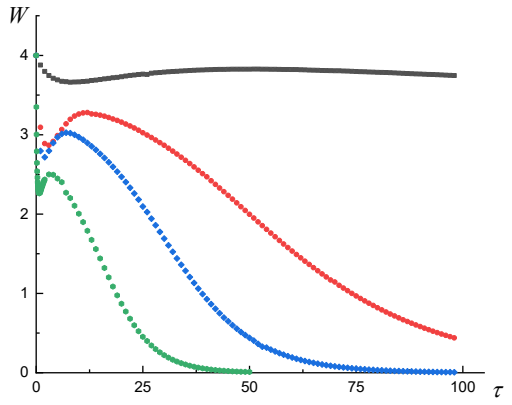

Figure 3. Change in the secondary structure depending on the time of hydrolysis at ε = 0.15 (■), ε = 2.4 (●), ε = 6 (♦), ε = 24 (●). W is the dimensionless concentration of secondary structures; τ is the dimensionless time.

Micellization caused by an increase in the concentration of β-casein leads to an increase in the β-structures [20]. Earlier it was shown that the aggregation of partially folded polypeptide chains of proteins leads to increased β-sheet signals and/or new β-sheet bands in the FTIR spectrum [21]. A similar effect was observed in our previous work [14], with the only difference that we studied the component Y formed by the fragments of a polypeptide chain rather than the whole protein. In contrast to the simplified concepts about protein hydrolysis by proteases, the hydrolysis of β-casein by trypsin under some conditions does not lead to monotonic degradation of the secondary structure (Fig. 3). The model proposed here shows that the most obvious effect of a decrease, a sharp increase, and then a gradual decline in the concentration of secondary structures can be expected at enzyme concentrations ε = 2.4 and 6. If the enzyme concentration is too low (ε = 0.15), this effect is practically unnoticeable, since the difference between the local minimum and maximum is small.

As well as in the previous report [14], we compared the results of the numerical modeling of the degradation *of* β-casein micelles by trypsin (scheme (1)) with the data on changes in the concentration of β-sheets determined by FTIR at 1633 cm^{-1} [12, 22]. Figure 4 shows good agreement between the obtained model curves and the experiment at three different enzyme concentrations, which were used in the experiments on β-casein degradation by trypsin performed with simultaneous registration of the FTIR spectra [14].

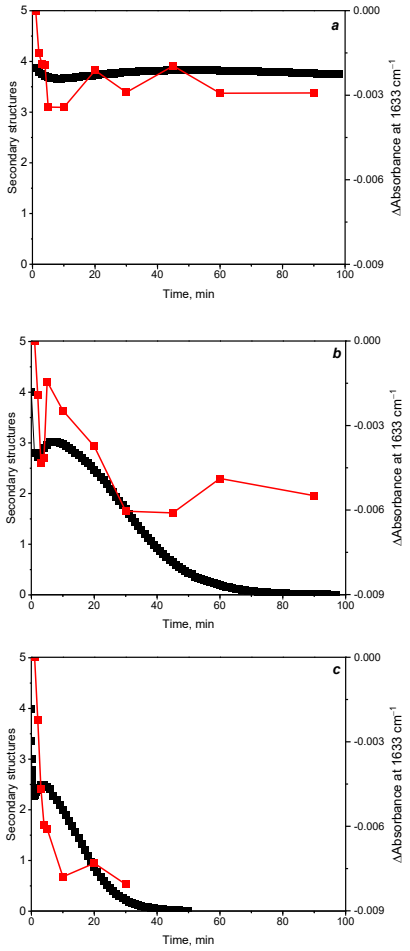

Figure 4. Comparison of the predicted change in the secondary structures (W, ■) during hydrolysis of β-casein micelles and absorption at 1633 cm^{-1} (■) corresponding to β-sheets [14]. Enzyme concentrations were as follows: ε = 0.15, $S_0/E_0 = 10^4$ (***a***); ε = 2.4, S_0/E_0 = 4000 (***b***); ε = 24, S_0/E_0 =500 (***c***).

Conclusions

The proposed kinetic model for the degradation of β-casein micelles can describe the changes in the concentrations of both the original micelle and its parts over time. In particular, the model well describes the accumulation of intermediate nanoparticles formed by the assembly of fragments of a β-casein polypeptide chain and capable of accumulating during hydrolysis and then slowly hydrolyzing. The model also well describes the experimentally observed effect of a nonmonotonic decrease in the concentration of secondary structures during hydrolysis. The range of enzyme concentrations at which there are observed a significant decrease, a sharp increase, and then a gradual decrease in the concentration of secondary structures during the process was determined.

Acknowledgements

This work was supported by both the Russian Foundation for Basic Research (project no. 20-53-46006, M. M. Vorob'ev)

and TÜBİTAK-2532 (no. 119N423, G. Güler). The work of the Russian team was supported by the Ministry of Science and Higher Education of the Russian Federation (agreement no. 075-00277-24-00).

Corresponding author

* E-mail: mmvor@ineos.ac.ru (M. M. Vorob'ev)

References

1. A. Shapira, Y. G. Assaraf, Y. D. Livney, *Nanomed.: Nanotechnol.*, *Biol. Med*., **2010**, *6*, 119–126. DOI: 10.1016/j.nano.2009.06.006
2. M. Li, R. Fokkink, Y. Ni, J. M. Kleijn, *Food Hydrocolloids*, **2019**, *96*, 653–662. DOI: 10.1016/j.foodhyd.2019.06.005
3. M. Bar-Zeev, Y. G Assaraf, Y. D. Livney, *Oncotarget*, **2016**, *7*, 23322–23334. DOI: 10.18632/oncotarget.8019
4. S. A. Forrest, R. Y. Yada, D. Rousseau, *J. Agric. Food Chem.*, **2005**, *53*, 8003–8009. DOI: 10.1021/jf0506611
5. M. M. Vorob'ev, V. S. Khomenkova, O. V. Sinitsyna, Levinskaya, D. Kh. Kitaeva, A. V. Kalistratova, M. S. Oshchepkov, L. V. Kovalenko, K. A. Kochetkov, *Russ. Chem. Bull.*, **2018**, *67*, 1508–1512. DOI: 10.1007/s11172-018-2248-7
6. M. M. Vorob'ev, O. V. Sinitsyna, *Int. Dairy J*., **2020**, *104*, 104652. DOI: 10.1016/j.idairyj.2020.104652
7. O. V. Sinitsyna, M. M. Vorob'ev, *Mendeleev Commun*., **2021**, *31*, 88–90. DOI: 10.1016/j.mencom.2021.01.027
8. O. V. Sinitsyna, M. M. Vorob'ev, *INEOS OPEN*, **2019**, *2*, 50–54. DOI: 10.32931/io1909a
9. G. Kegeles, *J. Phys. Chem.*, **1979**, *83*, 1728–1732. DOI: 10.1021/j100476a009
10. G. Kegeles, *Ind. J. Biochem. Biophys*., **1991**, *29*, 97–102.
11. J. E. O'Connell, V. Ya. Grinberg, C. G. de Kruif, *J. Colloid Interface Sci.*, **2003**, *258*, 33–39. DOI: 10.1016/S0021-9797(02)00066-8
12. M. M. Vorob'ev, V. Vogel, W. Mäntele, *Int. Dairy J*., **2013**, *30*, 33–38. DOI: 10.1016/j.idairyj.2012.12.002
13. M. M. Vorob'ev, K. Strauss, V. Vogel, W. Mäntele, *Food Biophys.*, **2015**, *10*, 309–315. DOI: 10.1007/s11483-015-9391-6
14. M. M. Vorob'ev, B. D. Açıkgöz, G. Güler, A. V. Golovanov, O. V. Sinitsyna, *Int. J. Mol. Sci*., **2023**, *24*, 3874. DOI: 10.3390/ijms24043874
15. A. V. Golovanov, M. M. Vorob'ev, *INEOS OPEN*, **2021**, *4*, 35–40. DOI: 10.32931/io2103a
16. W. Heller, W. J. Pangonis, *J. Chem. Phys*., **1957**, *26*, 498–506. DOI: 10.1063/1.1743332
17. S. H. Maron, P. E. Pierce, M. E. Elder, *J. Macromol. Sci*., *Part B: Phys.*, **1967**, *1*, 29–39. DOI: 10.1080/00222346708212738
18. J. Maurer, S. Haselbach, O. Klein, D. Baykut, V. Vogel, W. Mäntele, *J. Am. Chem. Soc.*, **2011**, *133*, 1134–1140. DOI: 10.1021/ja109699s
19. I. de la Arada, C. Seiler, W. Mäntele, *Eur. Biophys. J*., **2012**, *41*, 931–938. DOI: 10.1007/s00249-012-0845-1
20. D. A. Faizullin, T. A. Konnova, T. Haertle, Yu. F. Zuev, *Russ. J. Bioorg. Chem*., **2013**, *39*, 366–372. DOI: 10.1134/S1068162013040067
21. B. Shivu, S. Seshadri, J. Li, K. A. Oberg, V. N. Uversky, A. L. Fink, *Biochemistry*, **2013**, *52*, 5176–5183. DOI: 10.1021/bi400625v
22. A. Barth, *Biochim. Biophys. Acta*, *Bioenerg.*, **2007**, *1767*, 1073–1101. DOI: 10.1016/j.bbabio.2007.06.004